

# Floating Navigator Echo (FNAV) for In-Plane 2D Translational Motion Estimation

Yasser M. Kadah,<sup>1,2\*</sup> Ayman A. Abaza,<sup>2</sup> Ahmed S. Fahmy,<sup>3</sup> Abou-Bakr M. Youssef,<sup>2</sup> Keith Heberlein,<sup>1</sup> and Xiaoping P. Hu<sup>1</sup>

**A modification of the classical navigator echo (NAV) technique is presented whereby both 2D translational motion components are computed from a single navigator line. Instead of acquiring the NAV at the center of the  $k$ -space, a  $k_x$  line is acquired off-center in the phase-encoding ( $k_y$ ) direction as a floating NAV (FNAV). It is shown that the translational motion in both the readout and phase-encoding directions can be computed from this line. The algorithm used is described in detail and verified experimentally. The new technique can be readily implemented to replace classic NAV in MRI sequences, with little to no additional cost or complexity. The new method can help suppress 2D translational motion and provide more accurate motion estimates for other motion-suppression techniques, such as the diminishing variance algorithm. Magn Reson Med 51: 403–407, 2004. © 2004 Wiley-Liss, Inc.**

**Key words:** motion estimation; navigator echo; translational motion; motion artifact

Patient motion during MR acquisitions causes severe artifacts in the reconstructed images. In most such cases, the acquisition must be repeated, which adds to patient discomfort and decreases the efficiency of the MR system. Therefore, investigators have attempted to suppress such artifacts using various strategies, including patient motion restraints, motion monitoring during acquisition, and postprocessing methods (1). Among the most successful of these approaches are the navigator echo (NAV) technique and its variants (2–4). In the original formulation of this technique, one acquires an extra line in the center of  $k$ -space along the  $k_x$  or  $k_y$  directions to detect in-plane translational motion in that direction. One then compares the projection of the imaged region along this direction in which translational motion appears as a simple shift in the 1D signal. Hence, it is impossible to detect motion in both the readout and phase-encoding directions with a single NAV line.

In this work, we introduce a modified version of the original NAV technique that allows in-plane translational motion to be completely determined from a single navigator line. Instead of acquiring a line at the center of the

$k$ -space, we collect a floating navigator line as a slightly shifted line along the  $k_x$  direction that does not pass through the center of the  $k$ -space. The motion-estimation procedure consists of two steps. First, the motion along the  $x$ -direction of the line is determined in the same way as the regular NAV. Second, the phase corresponding to this motion is eliminated from the acquired line by appropriate phase compensation, and the phase of the center point is used to estimate the motion in the  $y$ -direction. We verified this new method with both computer simulations and real data, and analyzed its performance.

## MATERIALS AND METHODS

Translational motion manifests itself as an additional linear phase in the  $k$ -space along the direction of the motion, and thus it is generally expected that phase variations will be encountered in both the  $k_x$  and  $k_y$  directions. In order to characterize the translational motion completely, phase variations in both directions must be measured. In the classic NAV technique, this is done in two steps: first, the motion along  $k_x$  is measured, and then the motion along  $k_y$  is measured. This process reflects the fact that the NAV line passes through the center of  $k$ -space, which makes it impossible to measure phase variations along  $k_y$ . Here we consider the acquisition of an off-center (or floating) NAV (FNAV) line, as shown in Fig. 1. When a translational motion ( $\Delta x, \Delta y$ ) occurs, the signal from this line takes the form (5):

$$F_d(k_x, k_y) = e^{-j2\pi(k_x \Delta x + k_y \Delta y)} \iint f(x, y) \cdot e^{-j2\pi(k_x x + k_y y)} dx dy. \quad [1]$$

Here,  $F_d(k_x, k_y)$  is the navigator line defined as  $k_y = k_f$ , and  $f(x, y)$  is the spatial domain distribution of the imaged slices. We observe that this formulation has two parts: 1) the phase term representing the motion-induced linear phase, and 2) the integral representing the calculation of the undistorted  $k$ -space line (i.e., with no motion present). In an ideal scenario, once the same line is measured twice with motion in between, the linear fitting of the phase difference between the two lines should provide a linear term representing the motion in the  $x$ -direction and a constant term representing the motion in the  $y$ -direction. However, because this leads to phase wrapping and noise, this process is not practical. Therefore, we developed a two-step process to compute both components in a robust manner. The first step is to apply the inverse Fourier transformation to the navigator line. Instead of representing the simple projection along the  $x$ -direction, as in classical NAV, the Fourier transform (FT) of the FNAV repre-

<sup>1</sup>Biomedical Imaging Technology Center, Department of Biomedical Engineering, Emory University/Georgia Institute of Technology, Atlanta, Georgia.

<sup>2</sup>Biomedical Engineering Department, Cairo University, Giza, Egypt.

<sup>3</sup>Electrical Engineering Department, Johns Hopkins University, Baltimore, Maryland.

Grant sponsor: NIH; Grant numbers: RO1EB00331; RO1EB002009; Grant sponsors: International Electronics, Biomedical Division, Egypt; Georgia Research Alliance; Whitaker Foundation.

\*Correspondence to: Yasser M. Kadah, Ph.D., 531 Asburg Circle, Suite N305, Atlanta, GA 30322. E-mail: ymk@ieee.org

Received 2 June 2003; revised 8 September 2003; accepted 9 September 2003.

DOI 10.1002/mrm.10704

Published online in Wiley InterScience (www.interscience.wiley.com).

© 2004 Wiley-Liss, Inc.

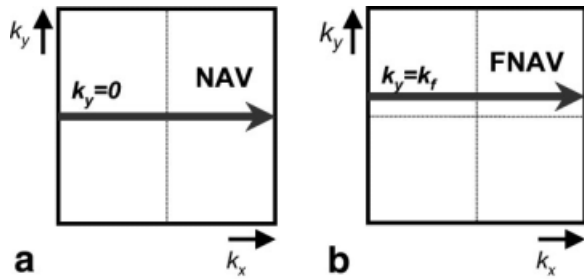


FIG. 1. Illustration of the acquisition method for (a) classic NAV and (b) FNAV.

sents the projection of the  $y$ -modulated version of the field of view (FOV) of the form:

$$f_{FNAV}(x) = e^{-j2\pi k_f \Delta y} \int f(x - \Delta x, y) \cdot e^{-j2\pi k_f y} dy. \quad [2]$$

Note that the form of the magnitude of this signal is not a function of  $\Delta y$ . Hence, the correlation of the magnitudes of two consecutive FNAV lines with motion in between is expected to have a peak that is only a function of  $\Delta x$ , just like classic NAV. Hence, the first step in our procedure to estimate the motion is to compute this displacement. Once this displacement is determined, we proceed to compensate for it in the FNAV line by multiplying by a linear phase with slope equal to the estimated  $\Delta x$ . In the second step, the displacement  $\Delta y$  is computed from the constant term in the least-squares linear fitting of the phase difference between the first FNAV and the compensated second FNAV around the center of the FNAV line. This takes care of noise and enables us to estimate residual subpixel displacement variations in the  $x$ -direction.

An important factor in the estimation of  $\Delta y$  is the possibility of phase wrapping in the  $k_y$  direction. Note that this displacement is computed from a single phase value given the position of the FNAV line ( $k_f$ ). Hence, it is possible in theory to have  $\Delta y$  displacements large enough to cause the phase term in Eq. [1] to wrap. In principle, the possible set of  $\Delta y$  values from a given phase measurement  $\phi$  is  $\{(\phi \pm 2n\pi)/2\pi k_f\}$ , where  $n$  is a positive integer. Consequently, a methodology to resolve the ambiguity of choosing  $n$  must be devised. The method we utilize is based on focusing methods that attempt to find the compensation phase value automatically by optimizing a focusing objective function in the resultant image (e.g., entropy or 1-norm) (6–8). In particular, a few values of  $n$  are used, and the focusing objective function is computed for each value. These functions are then compared to determine the correct value. This enables the use of such computationally expensive techniques given that the search space is substantially reduced. Moreover, for a NAV position that is close enough from the center, this might even be unnecessary given the small range of motion inside the magnet, and the fact that the maximum possible motion phase is a multiplication of the position in  $k$ -space by this range. After both components of the 2D translational motion are determined, the motion in the acquired data is compensated for by multiplying the  $k$ -space by the appro-

appropriate linear phase before applying the inverse Fourier transformation to compute the image.

Another important aspect of FNAV implementation is the selection of its position along the  $k_y$ -direction under different imaging conditions, such as the FOV and signal-to-noise ratio (SNR). This choice is constrained by the need to be far away from the pole at the center of  $k$ -space while at the same time maintaining a sufficient SNR to allow an accurate phase estimation. Based on our analysis in Appendix A, a suitable value is between  $4/\text{FOV}$  and  $14/\text{FOV} \text{ cm}^{-1}$ . A discussion of the noise model and a suggested practical selection methodology are also presented in the Appendix.

## RESULTS AND DISCUSSION

The proposed technique was implemented to correct simulated and experimental data. The simulations employed data generated using the exact form of a Shepp-Logan phantom (9) (i.e., sampling the exact FT expression of the phantom defined in Ref. 5). In these simulations, the mean and standard deviation (SD) of the motion estimation error for 100 random shift values within  $\pm 1$  cm are computed for a range of SNR values between 1 and 100. The simulation FOV used was  $24 \text{ cm} \times 24 \text{ cm}$ , corresponding to a matrix size of  $256 \times 256$ . The real data were acquired with a Siemens Magnetom Trio 3T MR system. Two sets of images of transverse slices were acquired in a normal human volunteer, with an induced 2D translational shift between acquisitions. An image with patient motion was obtained whereby half of the  $k$ -space was collected with the translational motion present. The imaging parameters were  $\text{TR}/\text{TE} = 150/4.9 \text{ ms}$ , flip angle =  $70^\circ$ , matrix =  $256 \times 224$ , and  $\text{FOV} = 23.6 \text{ cm} \times 27 \text{ cm}$ . The data were acquired in raw format and processed using the IDL development environment (Research Systems, Inc.).

The results of the simulation study indicated that FNAV motion estimation along the  $x$ -direction had exactly the same accuracy as NAV motion estimation in the same direction up to the pixel size of the transformed signal. This was determined by comparing the results from both the NAV and FNAV lines for the same motion to that of the true motion simulated. On the other hand, the estimation accuracy of the motion in the  $y$ -direction was found to depend on both the SNR and the position of the FNAV line, as predicted by the analysis in Appendix A. The mean and SD of the estimation error in that direction are presented in Fig. 2. In general, the results confirm the validity of the guidelines in Appendix A. The proposed range of FNAV positions appears to hold under low SNR values, whereas we can see that positions farther away suffer from significantly higher errors.

In the real-data experiment, the FNAV line was taken to be at position  $k_f = 10/\text{FOV} \text{ cm}^{-1}$ , in agreement with the analysis in Appendix A, and used as such for all experiments. Figure 3 shows an example of the acquired data. As can be seen, the corrected image using FNAV looks visually undistorted compared to the original. The correction made with NAV looks improved, but still sustains visible artifacts. The difference image demonstrates subtle differences between the FNAV-corrected and undistorted images, indicating the accuracy of the motion estimation.

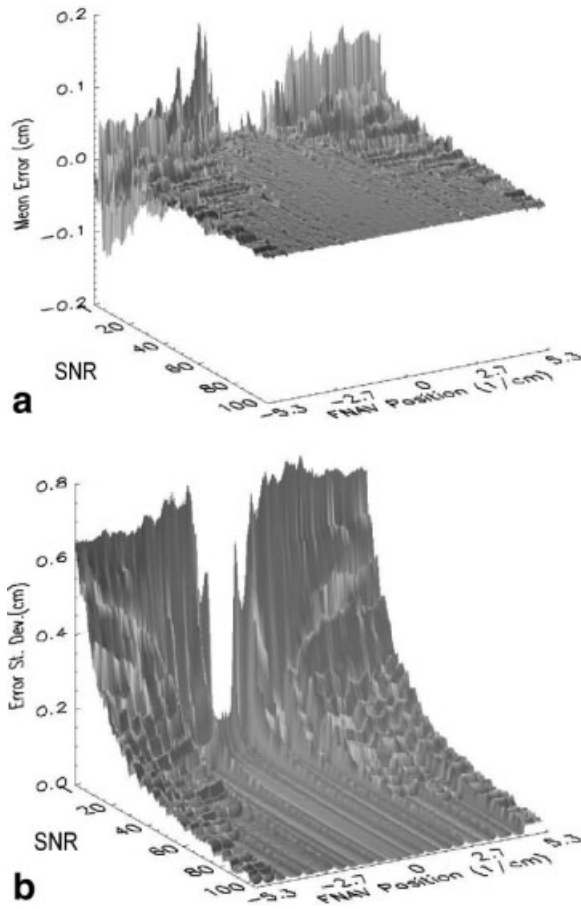


FIG. 2. Simulation results from estimating the translational motion along the phase-encoding direction obtained with FNAV: (a) mean of error between the estimated and true shifts, and (b) SD of the error.

To verify the selection criterion for the position of FNAV, we acquired two images with a 2D translational shift in between so that we could compare the FNAV results at different possible positions. In particular, we considered the FNAV position to be anywhere from  $-N_y/(2 \text{ FOV})$  to  $N_y/(2 \text{ FOV}) \text{ cm}^{-1}$ , which includes the NAV position at 0. The results of motion estimation along the readout direction are shown in Fig. 4a. As can be seen, FNAV can be used in a wide range of values, with exactly the same performance as NAV. The constant phase term for each FNAV line computed as the phase of the center point ( $k_x = 0$ ) of FNAV is shown in Fig. 4b, and the corresponding  $y$ -direction motion estimates are shown in Fig. 4c. As can be observed, the same conclusion we reached above for the  $x$ -direction motion estimation does not appear to be valid in the  $y$ -direction, where the small range of good values appears to be only around the center of  $k$ -space but not too close to the center. Within this range, the variations of the  $y$ -direction estimate were within  $\pm 0.5 \text{ mm}$  (0.4 pixel width), indicating an estimation error of even less than that even though a single point was used to compute the phase estimate. Using more points by estimating the constant term in a local fit around the center of FNAV provides an averaging mechanism whereby this error goes down as the square root of the number of points used in this estimation.

Note that the FNAV position used in this work ( $10/\text{FOV} \text{ cm}^{-1}$ ) falls in the middle of the range suggested in Appendix A. In fact, the whole range of positions appears to provide reasonable motion estimation accuracy in both the  $x$ - and  $y$ -directions. To illustrate the robustness of the suggested range, two studies were conducted whereby the root-mean-square (RMS) error for the difference image and the entropy focusing criterion of the corrected image were evaluated for  $y$ -direction motion estimation for different positions of FNAV. These studies used two real images acquired with a relative 2D shift in between to allow all possible positions of FNAV to be evaluated. The results are shown in Fig. 5a and b. As can be seen, the overall performance of FNAV is limited by the range of positions that allows the accurate estimation of  $y$ -direction motion. This range appears to include the suggested range of  $4\text{--}14/\text{FOV} \text{ cm}^{-1}$  for both criteria.

Two main applications can be proposed for the new method. The first is to use FNAV positioned appropriately to replace NAV in current imaging sequences. This requires minimal extra effort and no extra time (as compared to NAV) to add a  $y$ -gradient to position FNAV. This modification could be useful for online motion compensation strategies, such as the diminishing variance algorithm, for which a more accurate indication of motion is advantageous (10). The second application is to use FNAV as an overlapping line between subsequent acquisitions of  $k$ -space bands (as in fast spin-echo sequences). This is done by adding an extra line at the end of the band that overlaps the first line in the next band acquisition. Although this does not always guarantee that the  $y$ -direction motion will be estimated accurately, it allows a reduction of minimum TE and at the same time provides the same accuracy as NAV in estimating the  $x$ -direction motion. The extent of FNAV's usefulness in such applications remains to be investigated.

## CONCLUSIONS

In this work, a variant of the classic NAV technique was developed. The new method relies on acquiring an FNAV at a distance from the center of  $k$ -space. This enables both components of the 2D translational motion to be determined. FNAV motion estimation was demonstrated using real data, and was shown to be robust and simple to implement. Hence, it has the potential to enhance current MR applications that rely on classic NAV, with a minimal modification of existing sequences.

## APPENDIX A

### Selection of FNAV Position

$k$ -Space data collected in MRI are contaminated with white Gaussian noise in both the real and imaginary components. The effect of this noise on the magnitude and phase is rather complicated and depends on the actual magnitude of each  $k$ -space point, in addition to the characteristics of noise. This is likely to affect the most vulnerable part of the estimation procedure, i.e., estimating the motion in the  $y$ -direction from the phase of a single point. In the worst-case scenario for this estimation procedure, the constant component of the phase is estimated using

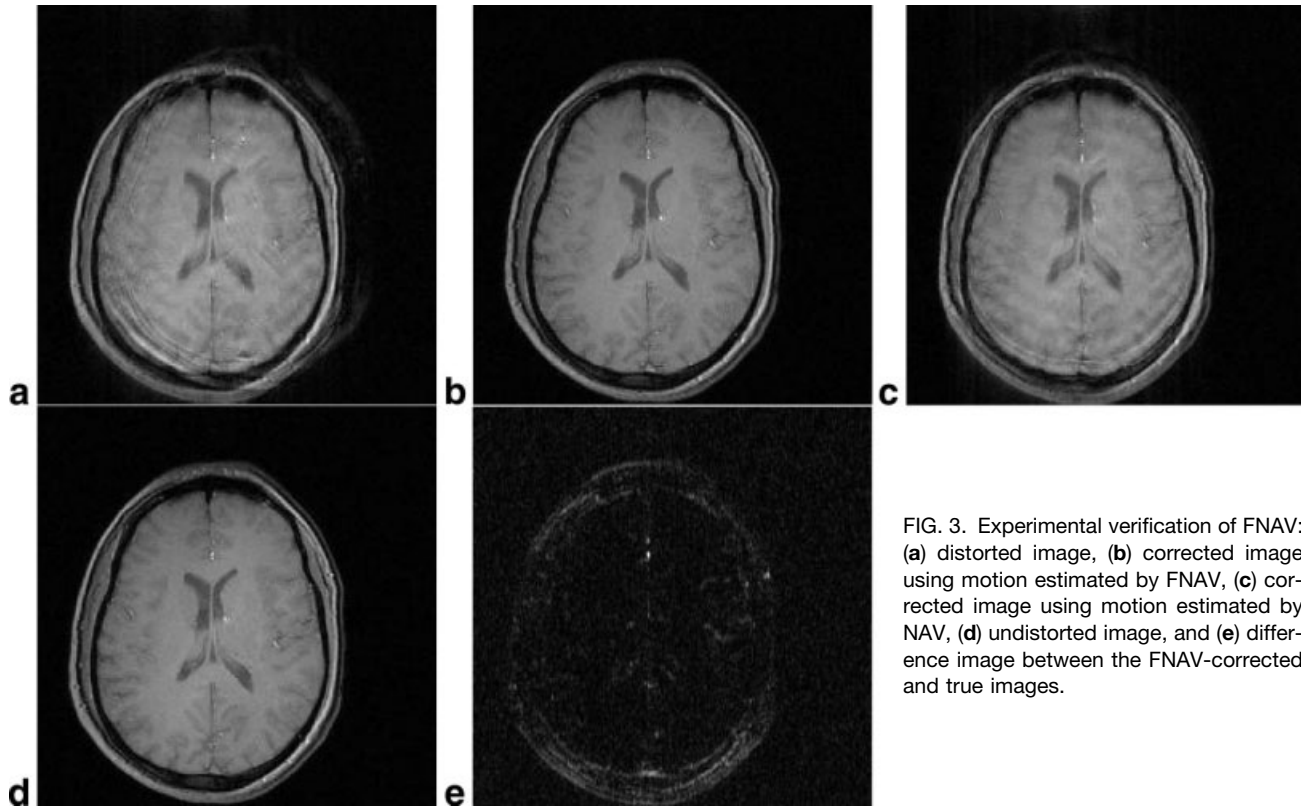


FIG. 3. Experimental verification of FNAV: (a) distorted image, (b) corrected image using motion estimated by FNAV, (c) corrected image using motion estimated by NAV, (d) undistorted image, and (e) difference image between the FNAV-corrected and true images.

only one point at the center of the FNAV. Gudbjartsson and Patz (11) presented a review of the literature describing the magnitude and phase probability distributions. In particular, the probability distribution of phase noise,  $\Delta\theta = \theta - \theta_{true}$  takes the form:

$$p(\Delta\theta) = \frac{1}{2\pi} e^{-A^2/2\sigma^2} \cdot \left[ 1 + \frac{A}{\sigma} \sqrt{2\pi} \cdot \cos(\Delta\theta) \times e^{A^2 \cos^2(\Delta\theta)/2\sigma^2} \cdot \frac{1}{\sqrt{2\pi}} \int_{-\infty}^{A \cos(\Delta\theta)/\sigma} e^{-x^2/2} dx \right]. \quad [I.1]$$

Here,  $A$  is the true magnitude of the data point, and  $\sigma$  is the noise SD in each of the quadrature components. As can be observed from this expression, the noise probability distribution is a function of the SNR of the point of interest. When the SNR, defined as  $(A/\sigma)$ , is sufficiently large, the above expression becomes very close to a zero-mean Gaussian distribution with an SD given by  $(\sigma/A)$  (11). In fact, this is a good approximation even for SNR values down to unity. For our FNAV motion estimation problem, the phase is estimated from the phase difference of two points that each have the above noise probability distribution. This translates to an SD of  $(2\sigma/A)$  for points with high SNR. Given that the shift estimate is computed from the phase difference divided by the FNAV location, the amount of phase noise is divided by how far the FNAV line is from the center of the  $k$ -space. Nevertheless, the true magnitude of a  $k$ -space point also changes with its location, the characteristics of physical slice being imaged, and the imaging parameters (e.g., the FOV)

used in the experiment. Consequently, it is rather difficult to derive a general criterion for the optimum selection of the FNAV line position.

This problem bears some resemblance to the problem of selecting the radius of the orbital NAV (ONAV), where a balance between good SNR (best near the center of  $k$ -space) and accuracy or detail (worst near the center of  $k$ -space) must be considered (12). The empirical selection used for the ONAV problem was five times the inverse of the FOV. Here, the selection of a point that is too close to the center of the  $k$ -space is not recommended, because the estimation formula has a pole at the center of  $k$ -space. On the other hand, the  $k$ -space magnitude falls off quickly with increasing distance from the center of  $k$ -space. Unlike ONAV, where the presence of a low  $k$ -space point on the orbital trajectory does not significantly affect accuracy, the FNAV estimation procedure must ensure that the  $k$ -space point used to estimate the  $y$ -direction motion has sufficient SNR. We used a practical procedure to allow the determination of a suitable location, whereby two NAV lines per slice were acquired along the  $k_y$  direction in the preparation phase of the imaging sequence. The imaging parameters for these acquisitions (such as the FOV and the matrix size) were taken as those of the subsequent imaging procedure. The imaging parameters for the second acquisition were slightly changed to shift the FOV relative to that used in the first acquisition by a known amount in the  $y$ -direction. The  $y$ -motion estimates based on the phase difference between the respective points on the two NAV lines were computed to represent FNAV lines at different positions. The FNAV position is selected as the median location among the subset of points with the smallest

shift estimation error. Even though the actual experiment relies on the more accurate least-squares fit, the error in the center point represents a fast and reliable estimate of the local SNR of a particular FNAV position. In our experiments, the most reliable range was anything between  $4/\text{FOV}$  and  $14/\text{FOV cm}^{-1}$ , which provides an excellent balance between being sufficiently far away from the center of the  $k$ -space and maintaining a suitable  $k$ -space magnitude to provide a robust estimate of phase.

As regards the effect of noise on the estimation of the  $x$ -direction motion, the magnitude information used to compute this estimate belongs to the Rician distribution. For sufficiently high SNR values, this distribution again becomes very similar to the Gaussian distribution. The main difference here is that the estimate is computed from all points on the FNAV line, rather than from one or a few points for the  $y$ -direction. Hence, in general the new method is expected to be robust.

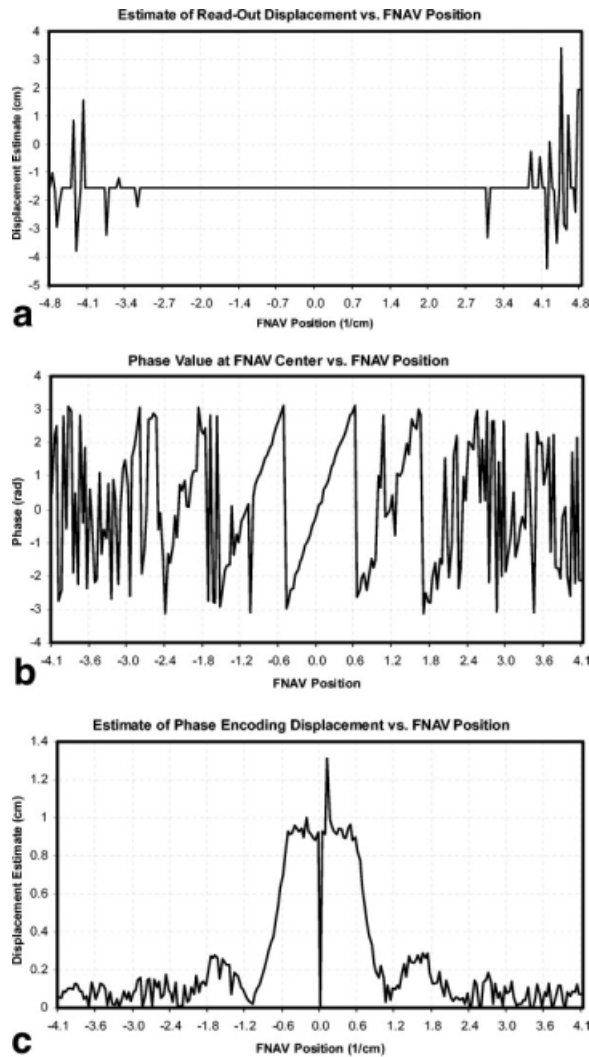


FIG. 4. Experimental results from FNAV motion estimation for different FNAV line positions. **a**: The estimated  $x$ -direction shift. **b**: Difference phase at the center of FNAV. **c**: The estimated  $y$ -direction shift based on the difference phase in **b**.

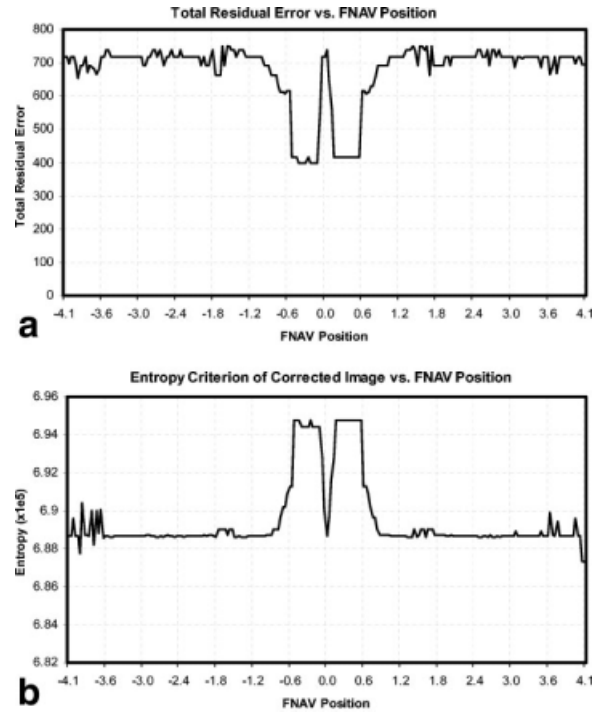


FIG. 5. The performance of the FNAV technique vs. the FNAV position, as evaluated by the RMS of the difference image in **a**, and the entropy focusing criterion of the corrected image in **b**.

## REFERENCES

1. Zoroofi RA, Sato Y, Tamura S, Naito H, Tang L. An improved method for MRI artifact correction due to translational motion in the image plane. *IEEE Trans Med Imaging* 1995;14:471–479.
2. Ehman RL, Felmlee JP. Adaptive technique for high definition MR imaging of moving structures. *Radiology* 1989;173:255–263.
3. McGee KP, Felmlee JP, Manduca A, Riederer SJ, Ehman RL. Rapid autocorrection using prescan navigator echoes. *Magn Reson Med* 2000; 43:583–588.
4. Welch EB, Manduca A, Grimm RC, Ward HA, Jack CR. Spherical navigator echoes for full 3D rigid body motion measurement in MRI. *Magn Reson Med* 2002;47:32–41.
5. Bracewell RN. *The Fourier transform and its applications*. 2nd ed. New York: McGraw Hill; 1986.
6. Hedley M, Yan H, Rosenfeld D. A modified Gerchberg-Saxton algorithm for one-dimensional motion artifact motion artifact correction in MRI. *IEEE Trans Signal Processing* 1991;39:1428–1433.
7. Kadah YM, Hu X. Automatic suppression of spatially variant translational motion artifacts in magnetic resonance imaging. In: *Proceedings of the IEEE International Conference on Image Processing*, Chicago, 1998. p 24–28.
8. Atkinson D, Hill DLG, Stoye PNR, Summers PE, Keevil SF. Automatic correction of motion artifacts in magnetic resonance images using an entropy focusing criterion. *IEEE Trans Med Imaging* 1997;6:903–910.
9. Shepp LA, Logan BF. Reconstructing interior head tissue from x-ray transmissions. *IEEE Trans Nucl Sci* 1974;NS-21:228–236.
10. Sachs TS, Meyer CH, Irarrazabal P, Hu BS, Nishimura DG, Macovski A. The diminishing variance algorithm for real-time reduction of motion artifacts in MRI. *Magn Reson Med* 1995;34:412–422.
11. Gudbjartsson H, Patz S. The Rician distribution of noisy MRI data. *Magn Reson Med* 1995;34:910–914.
12. Fu ZW, Wang Y, Grimm RC, Rossman PJ, Felmlee JP, Riederer SJ, Ehman RL. Orbital navigator echoes for motion measurements in magnetic resonance imaging. *Magn Reson Med* 1995;34:746–753.